

On the Capon's Method Application in Time-Frequency Analysis

L. Jubiša Stanković, Vesna Popović, Miloš Daković

Abstract—Capon's method is widely used in the literature in array signal processing and spectral analysis. Recently, this method has been extended to the time-frequency analysis. The topic of this paper is to compare the standard spectrogram and its Capon's counterpart, with respect to the several basic parameters: instantaneous frequency estimation, distribution concentration, and resolution of two close components. The analysis is generalized to the distributions from the Cohen class and distributions that take into account phase nonlinearity.

I. INTRODUCTION

TIME-frequency analysis is used in order to get a time distribution of the signal's spectral content [6]. The simplest method for this analysis is based on the short-time Fourier transform (STFT), which is a straightforward extension of the Fourier transform. However, the STFT performance is highly dependent on the window used for signal localization. In order to improve time-frequency concentration, various other representations are defined [6]. One research direction is in improving signal's concentration in time-frequency plane by increasing the order of representation [4], [15], [16]. Another direction is in keeping important property of transform linearity with respect to the signal, but introducing polynomial forms with respect to the lag coordinate [7], [14]. The third research direction, with the same goal, is in defining signal adaptive representations [1], [2], [3], [8].

An adaptive approach, used to improve the concentration and resolution of the time-frequency representations, is based on the Capon's adaptive filtering [5]. The Capon's form, originally proposed as an array-processing technique, is quite efficient spectral

analysis tool [9], [12], [17], [18]. It is used in order to improve both the resolution and estimation accuracy. Here we will analyze the performance of Capon based method in time-frequency analysis as it was proposed and presented in [11], [13]. Results are compared with the ones that can be obtained by using the standard or smoothed spectrogram for the same purpose. Several straightforward modifications of the spectrogram forms are presented just to illustrate the conclusions.

This letter contains an overview of the basic definitions of the Capon's method in Section II. Relation between Capon's and standard spectrogram, with respect to the instantaneous frequency estimation, concentration, and resolution of two close components is studied in Section III. Numerical examples illustrate the theoretical conclusions.

II. BASIC MODELS AND DEFINITIONS

The Capon's filtering method applied to N samples of a noisy signal $x(t)$, denoted in vector form as

$$\mathbf{x}(t)=[x(t)x(t+1)x(t+2)\dots x(t+N-1)]^T, \quad (1)$$

results in the distribution

$$S_{Capon}(t, \omega) = \frac{1}{\mathbf{a}^*(\omega)\hat{\mathbf{R}}_{\mathbf{x}}^{-1}\mathbf{a}(\omega)}, \quad (2)$$

where $*$ denotes Hermitian transpose and:

$$\mathbf{a}(\omega) = [1 e^{i\omega} e^{i\omega 2} \dots e^{i\omega(N-1)}]^T, \quad (3)$$

$$\hat{\mathbf{R}}_{\mathbf{x}} = E\{\mathbf{x}(t)\mathbf{x}^*(t)\}. \quad (4)$$

In practice, the autocorrelation matrix $\hat{\mathbf{R}}_{\mathbf{x}}$ is estimated by:

$$\hat{\mathbf{R}}_{\mathbf{x}}(t, K) = \frac{1}{K} \sum_{p=0}^{K-1} \mathbf{x}(t+p)\mathbf{x}^*(t+p) + \rho\mathbf{I}$$

$$= \frac{1}{K} \mathbf{Q} \mathbf{Q}^* + \rho \mathbf{I}, \quad (5)$$

where \mathbf{I} is the identity matrix used for regularization, \mathbf{Q} is the matrix whose columns are signal vectors $\mathbf{x}(t+p)$, $p = 0, 1, \dots, K-1$.

III. RELATION BETWEEN THE STANDARD SPECTROGRAM AND THE CAPON'S FORM

Inversion of the autocorrelation matrix (5) can be done by using:

$$\begin{aligned} & \left(\frac{1}{K} \mathbf{Q} \mathbf{Q}^* + \rho \mathbf{I} \right)^{-1} = \\ & \frac{1}{\rho} \left[\mathbf{I} - \mathbf{Q} \left(\mathbf{I} + \frac{\mathbf{Q}^* \mathbf{Q}}{K\rho} \right)^{-1} \mathbf{Q}^* \frac{1}{K\rho} \right]. \end{aligned} \quad (6)$$

From (1) and (6) follows:

$$\begin{aligned} S_{Capon}(t, \omega) &= \\ & \frac{1}{\mathbf{a}^*(\omega) \frac{1}{\rho} \left[\mathbf{I} - \mathbf{Q} \left(\mathbf{I} + \frac{\mathbf{Q}^* \mathbf{Q}}{K\rho} \right)^{-1} \mathbf{Q}^* \frac{1}{K\rho} \right] \mathbf{a}(\omega)} \\ &= \frac{\rho}{N - \mathbf{STFT}(\omega, t) (K\rho \mathbf{I} + \mathbf{Q}^* \mathbf{Q})^{-1} \mathbf{STFT}^*(\omega, t)} \end{aligned} \quad (7)$$

where $\mathbf{STFT}(\omega, t) = \mathbf{a}^*(\omega) \mathbf{Q}$ is a vector whose elements are $STFT(\omega, t+p) = \mathbf{a}^*(\omega) \mathbf{x}(t+p)$, $p = 0, 1, \dots, K-1$. For $K=1$ when $\mathbf{Q} = \mathbf{x}(t)$ we get:

$$S_{Capon1}(t, \omega) = \frac{\rho}{N - (E_x + \rho)^{-1} |STFT(\omega, t)|^2}, \quad (8)$$

where $E_x = \sum_{p=0}^{N-1} |x(t+p)|^2$ is the energy of $\mathbf{x}(t)$ and $STFT(\omega, t) = \mathbf{a}^*(\omega) \mathbf{x}(t)$ is the standard STFT, while $|STFT(\omega, t)|^2$ is the standard spectrogram.

The Capon's form can be written by using eigenvalues decomposition of the autocorrelation matrix $\hat{\mathbf{R}}_{\mathbf{x}}(t, K)$ (or singular values decomposition of the signal matrix \mathbf{Q}) as

$$\begin{aligned} \hat{\mathbf{R}}_{\mathbf{x}}(t, K) &= \\ \frac{1}{K} \mathbf{Q} \mathbf{Q}^* + \rho \mathbf{I} &= \frac{1}{K} (\mathbf{U} \mathbf{S} \mathbf{V}^*)^* (\mathbf{U} \mathbf{S} \mathbf{V}^*) + \rho \mathbf{I} \\ &= \frac{1}{K} \mathbf{V} \mathbf{\Lambda} \mathbf{V}^* + \rho \mathbf{I}, \end{aligned}$$

where \mathbf{U} and \mathbf{V} are left and right singular value decomposition matrices of \mathbf{Q} , \mathbf{S} is matrix of corresponding singular values of \mathbf{Q} , while $\mathbf{\Lambda} = \mathbf{S}^2$ is the eigenvalues matrix of $\hat{\mathbf{R}}_{\mathbf{x}}(t, K)$. By using this decomposition we can write

$$\hat{\mathbf{R}}_{\mathbf{x}}^{-1}(t, K) = \frac{1}{\rho} \left[\mathbf{I} - \sum_{p=0}^{K-1} \left(1 + \frac{\rho K}{\lambda_p} \right)^{-1} \mathbf{V}_p \mathbf{V}_p^* \right]$$

where \mathbf{V}_p are eigenvectors and λ_p are eigenvalues of $\hat{\mathbf{R}}_{\mathbf{x}}(t, K)$. The Capon's form then reads

$$S_{CaponK}(t, \omega) = \frac{\rho}{\mathbf{N} - \sum_{p=0}^{K-1} \frac{\lambda_p}{K\rho + \lambda_p} SPEC_{V_p}(\omega, t)}$$

where $SPEC_{V_p}(\omega, t)$ are the spectrograms of the eigenvectors.

Special cases:

1. When $K\rho \gg \lambda_{\max}$ then $\lambda_p / (K\rho + \lambda_p) \rightarrow \lambda_p / (K\rho)$ producing

$$\begin{aligned} S_{CaponK}(t, \omega) &= \frac{\rho}{\mathbf{N} - \frac{1}{K\rho} \sum_{p=0}^{K-1} \lambda_p SPEC_{V_p}(\omega, t)} = \\ &= \frac{\rho}{\mathbf{N} - \frac{1}{K\rho} \sum_{p=0}^{K-1} SPEC_x(\omega, t+p)} \end{aligned}$$

since $\sum_{p=0}^{K-1} \lambda_p \mathbf{V}_p \mathbf{V}_p^* = \mathbf{Q} \mathbf{Q}^*$, what reduces to the smoothed standard spectrogram.

2. When $K\rho \rightarrow 0$, $\lambda_p \neq 0$, $p = 0, 1, \dots, K-1$ we get:

$$S_{CaponK}(t, \omega) = \frac{\rho}{\mathbf{N} - \sum_{p=0}^{K-1} SPEC_{V_p}(\omega, t)} \quad (9)$$

When the signal $x(t)$ contains well separated FM components $x(t) = \sum_{m=1}^M x_m(t) = \sum_{m=1}^M A_m \exp(j\phi_m(t))$, as in [11], [13], then the eigenvectors are proportional to the signal components resulting in a linear combination of the spectrograms of the components with normalized amplitudes:

$$S_{CaponK}(t, \omega) = \frac{\rho}{\mathbf{N} - \sum_{m=1}^M \frac{SPEC_{x_m}(\omega, t)}{A_m^2}} \quad (10)$$

A. Instantaneous Frequency (IF) estimation

The spectrogram and the Capon's spectrogram have the same performance with respect to the IF estimation for one component signal.

Proof: Denote the absolute value of the STFT by a general real-valued function $f(\omega)$ that has maximum at $\omega = \omega_0$. Function of the form (8)

$$g(\omega) = \frac{a}{b - f^2(\omega)},$$

has the maximum at the same position (assuming that $b > f^2(\omega)$), since denominator in $g(\omega)$ reaches smallest value for greatest $f^2(\omega)$. Therefore, the spectrogram $|STFT(\omega, t)|^2$ and the Capon's form defined by (8) have maxima at the same position. Since the IF is estimated based on the position of maximum, $\omega_i(t) = \arg\{\max_{\omega}\{|STFT(\omega, t)|^2\}\}$, both of these distributions behave the same with respect to the IF estimation.

Note 1: With respect to the IF estimation, the spectrogram and $S_{Capon}(t, \omega)$ behave in the same way for multicomponent signals well separated in time-frequency plane, as they were in [11], [13].

B. Concentration

Capon's spectrogram (8) can look much better concentrated in the time-frequency plane than the standard spectrogram.

Proof: Assume again that $f(\omega)$ symbolizes absolute value of the STFT, while $g(\omega) = a/(b - f^2(\omega))$ symbolizes the Capon's form (8). If the regularization parameter b is appropriately chosen, so that $b = \max(f^2(\omega)) + \beta$, where $\beta \rightarrow 0+$, we get $g(\omega) \rightarrow +\infty$ at $\omega = \omega_0$, where ω_0 is the position of the maximum of $f(\omega)$. Thus, if we normalize the values of $g(\omega)$ by $g(\omega_0)$, we will get an ideally concentrated function $g(\omega) = 1$ for $\omega = \omega_0$, and $g(\omega) \rightarrow 0+$ for all other ω , see Fig.1a) and b).

As long as $b = \max(f^2(\omega)) + \beta$, with $\beta > 0$, the Capon's spectrogram looks better concentrated. In the limit case, when $\beta \rightarrow \infty$, then

$$g(\omega) = \frac{a}{b - f^2(\omega)} = \frac{a}{b} (1 + f^2(\omega)/b),$$

i.e., the Capon's spectrogram will be just a scaled version of the standard spectrogram.

We can define a very simple, almost ideally concentrated, distribution based on the spectrogram, as

$$S_C(\omega, t) = \frac{\mu}{1 - |STFT(\omega, t)|^2 / [M(t)(1 + \mu)]}, \quad (11)$$

where $M(t) = \max_{\omega}\{|STFT(\omega, t)|^2\}$, with μ quite small, for example $\mu = 0.001$. Then, we will get almost ideally concentrated distribution: $S_C(\omega, t) = 1$ at $\omega_i(t) = \arg\max_{\omega}\{|STFT(\omega, t)|^2\}$, and $S_C(\omega, t) = 0$ elsewhere. Here, all parameters are defined without any reference to the physical meaning of the parameters in the Capon's derivation [11], [13]. For multicomponent signals this distribution will produce almost ideally concentrated components, if they are of the same amplitude. Components with amplitudes smaller than the maximal one will be less concentrated, but still better than in the standard spectrogram. Note that the normalization may cause large changes in components amplitudes.

Example 1: Consider signal

$$x(t) = \exp[-2t^2 + j32\pi \sin(t\pi)]$$

within $|t| \leq 1$. The spectrogram of this signal, calculated by using the Hanning window of the width $N = 16$ zero-padded up to 256 samples, is shown in Fig.1c. Modified spectrogram, calculated according to (11) with $\mu = 0.001$, is shown in Fig.1d. The last one is almost ideally concentrated along the IF.

C. Resolution of two close components

For signal with two components $s(t) = \exp(j\omega_0 t) + \exp(j(\omega_0 + \varepsilon)t)$ we can resolve components from the standard spectrogram at an appropriate time instant.

Proof: Both Capon's and standard spectrogram behave as

$$|STFT(\omega, t)|^2 = |STFT_1(\omega, t) + STFT_2(\omega, t)|^2, \quad (12)$$

where $STFT_1(\omega, t)$ and $STFT_2(\omega, t)$ are the STFTs of signal components. They are related to the Fourier transform (FT) of the lag window $W(\omega)$ as

$$STFT_1(\omega, t) = W(\omega - \omega_0)e^{-j(\omega - \omega_0)t}$$

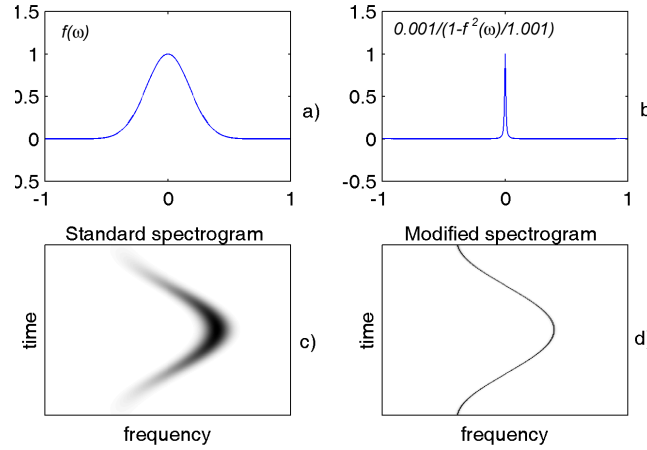


Fig. 1. Illustration of the relation between Capon's and standard spectrogram: a) Illustration of a standard spectrogram at a given instant, b) Illustration of the corresponding modified spectrogram, c) Standard spectrogram of a sinusoidally modulated signal, d) Modified spectrogram corresponding to the Capon's form.

$$STFT_2(\omega, t) = W(\omega - (\omega_0 + \varepsilon))e^{-j(\omega - \omega_0)t}e^{j\varepsilon t}.$$

Thus we get

$$|STFT(\omega, t)|^2 = |W(\omega - \omega_0) + e^{j\varepsilon t}W(\omega - \omega_0 - \varepsilon)|^2.$$

Independently on the lag window width, there is an instant where $\varepsilon t = (2n + 1)\pi$ when,

$$|STFT(\omega, t)|^2 = |W(\omega - \omega_0) - W(\omega - \omega_0 - \varepsilon)|^2. \quad (13)$$

Since the FT of window function $W(\omega) = W(-\omega)$ is symmetric, then $|STFT(\omega_0 + \frac{\varepsilon}{2}, t)|^2 = 0$ as long as we can find a point where $\varepsilon t = (2n + 1)\pi$. Thus, as long as we can find a zero value (or a minimum), anywhere in time, between two components in the spectrogram at $\omega = \omega_0 + \frac{\varepsilon}{2}$, there will exist two picks in the spectrogram.

Accordingly, we can define a very simple modified spectrogram, with almost ideal resolution, for any window width:

$$S_H(\omega, t) =$$

$$\min\{|STFT(\omega, t + p)|^2 : 0 \leq p \leq K - 1\}, \quad (14)$$

$$S_{IH}(\omega, t) = \frac{\mu}{1 - S_H(\omega, t)/[M_H(t)(1 + \mu)]}, \quad (15)$$

where $M_H(t) = \max_{\omega}\{S_H(\omega, t)\}$.

Relation (14) follows from the fact that (12) reaches minimum at $\exp(j\varepsilon t) = -1$.

Example 2: Consider discrete-time signal with two close components:

$$x(n) = \exp(j\frac{2\pi}{16}1.375n) + \exp(j\frac{2\pi}{16}1.5n).$$

The spectrogram is calculated by using the Hanning window of the width $N = 16$ zero-padded up to 256 samples (16 times interpolation). Width of one signal component calculated by Hanning window is approximately 3 samples, or 48 samples after the interpolation, Fig.2a). Thus, after the interpolation the components are only two samples apart (at $k_1 = 1.375 \times 16 = 22$, and $k_2 = 1.5 \times 16 = 24$). Spectrogram is shown in Fig.2a), the spectrogram calculated by (14), with $K = 128$, is shown in Fig.2b), while the result obtained by (15) is given in Fig.2c). Components are shifted in frequency for 128 samples (corresponding to negative frequencies). We can see that the highly concentrated distribution (15), corresponding to the Capon's form, can be obtained only if the components can be separated in (14). The components are highly biased with respect to the true frequency values at $k_1 = 128 + 22$, and $k_2 = 128 + 24$. Bias follows

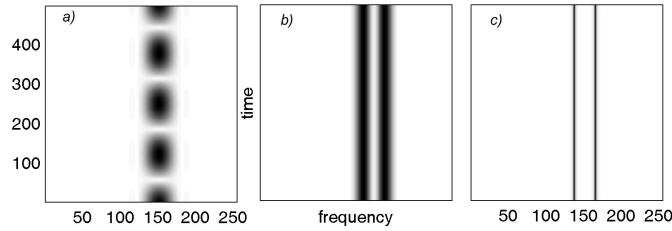


Fig. 2. Resolution of two close components: a) Standard STFT absolute value, b) Spectrogram $S_H(\omega, t)$ obtained from the standard spectrogram(a) by using relation (14), c) Modified spectrogram calculated by using (15).

from the shifted maxima in (13).

D. Generalization

The above forms can be generalized in two ways:

(a) For application on signals with arbitrary frequency varying components, all the previous results can be generalized by using [9], [10], [13]:

$$\mathbf{a}_t(\omega) = [1 e^{i\Delta^{[1]}\varphi(t)} e^{i\Delta^{[2]}\varphi(t)} \dots e^{i\Delta^{[L-1]}\varphi(t)}]^T, \quad (16)$$

where $\Delta^{[k]}\varphi(t) = \varphi(t+k) - \varphi(t)$, $k = 1, \dots, L-1$. This form would be efficient in the analysis of linear (or generally polynomial) frequency modulated signals.

(b) By using the local autocorrelation function vector $\mathbf{r}_t(\tau)$:

$$\mathbf{r}_t(\tau) = [r_t(0) r_t(1) r_t(2) \dots r_t(N-1)]^T, \quad (17)$$

with elements $r_t(p) = \sum \varphi(p, l)x(t+l+p)x^*(t+l-p)$, instead of the signal vector $\mathbf{x}(t)$, we can apply all the previous forms to the quadratic distributions from the Cohen class. Here $\varphi(p, l)$ denotes kernel in time-lag domain.

For example, the modified Choi-Williams distribution (CWD) can be obtained by using:

$$CW_C(\omega, t) = \frac{\mu}{1 - CW^2(\omega, t) / [M_{CW}(t)(1 + \mu)]},$$

with $M_{CW}(t) = \max_{\omega} \{CW^2(\omega, t)\}$.

Example 3: Consider the CWD with kernel:

$$\varphi(t, \tau) =$$

$$FT_{\theta} \{ \exp(-45\theta\tau^2) \} \text{ for } -1 \leq |\theta|, |\tau| < 1$$

sampled at 1/128. Signal was of the form:

$$x(t) = \nu(t) + e^{-9(t-\frac{1}{2})^2} \left(e^{j(500t^2+512\pi t)} + e^{j(-500t^2+512\pi t)} \right),$$

motivated by an example in [11]. Signal is sampled at 1/1024. Standard deviation of Gaussian noise $\nu(t)$ was 0.1. The CWD is calculated by using the eigenvalues-kernel decomposition. Signal is zero-padded four times before the Fourier transform calculation for each eigenvector. The CWD is shown in Fig.3a). The modified CWD by using the absolute maximum in the entire time-frequency plane with $\mu = 0.1$, is shown in Fig.3b). Modified CWD, by using maxima for each time instant and $\mu = 0.01$, is presented in Fig.3c). The last distribution is multiplied by the total signal spectra power density function, in order not to show the regions where there is no signal.

The analysis presented in this section can be used for a simplified calculation of the Capon's method, without using autocorrelation matrix. From (9) and (10) we can see that the Capon's distribution is directly related to the sum of spectrograms of the autocorrelation matrix eigenvectors. For multicomponent well separated signals, in time-frequency plane, the eigenvectors are proportional to the signal components. Thus, the Capon's form can be obtained from the normalized sum of spectrograms of signal components.

IV. CONCLUSION

The Capon's and standard forms of time-frequency representations are considered and

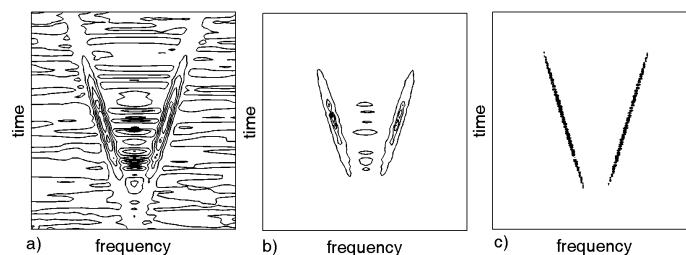


Fig. 3. Time-frequency representations based on the Choi-Williams distribution: a) Choi-Williams distribution, b) Modified Choi-Williams distribution by using the absolute maximum, c) Modified Choi-Williams distribution by using maxima for each time instant. Distribution is multiplied by the total signal power spectra density function.

compared with respect to several basic properties: instantaneous frequency estimation, distribution concentration, and resolution of two close components. For the monocomponent signals and multicomponent signals with well separated components, as they were considered in literature for time frequency analysis, the Capon's form produce exactly the same results as the standard one with respect to the first and the third property, while it can look much more concentrated in the time-frequency plane. Simple modifications of the standard spectrogram are proposed in order to illustrate these conclusions. The analysis is generalized to the distributions from the Cohen class, and to the distributions that take into account phase nonlinearity.

REFERENCES

- [1] F. Auger, P. Flandrin: "Improving the readability of time-frequency and time-scale representations by the reassignment method", *IEEE Trans. on Signal Processing*, vol-43, no.5, May 1995, pp.1068-1089.
- [2] S. Barbarossa: "Analysis of multicomponent LFM signals by a combined Wigner-Hough transform", *IEEE Trans. on Signal Processing*, vol.43, no.6, June 1995, pp.1511-1515.
- [3] A. Belouchrani, M.G. Amin: "Time-frequency MUSIC", *IEEE Signal Processing Letters*, vol-6, no.5, May 1999, 109-110.
- [4] B. Boashash: "Estimating and interpreting the instantaneous frequency of a signal-Part 1: Fundamentals", *Proc. IEEE*, vol-80, no.4, April 1992, pp.519-538.
- [5] J. Capon, "High-resolution frequency - wavenumber spectrum analysis", *Proceedings of IEEE*, vol. 57, no. 8, 1969, pp. 1408-1418.
- [6] L.Cohen, *Time-frequency analysis*, Prentice-Hall, 1995.
- [7] V. Katkovnik, "A new form of the Fourier transform for the time-varying frequency estimation", *Signal Processing*, v. 47, 1995, pp. 187-200.
- [8] V.Katkovnik, L.J.Stanković: "Instantaneous frequency estimation using the Wigner distribution with varying and data-driven window length", *IEEE Trans. on Signal Processing*, vol.46, no.9, Sept. 1998, pp.2315-2325.
- [9] V.Katkovnik: "Adaptive LPA-beamforming for moving sources", *Signal Processing*, Feb. 2003.
- [10] V.Katkovnik, L.J.Stanković, "High-resolution Data-adaptive time-frequency analysis", *IEEE Int. Conference on Electronics, Circuits and Systems*, ICECS 2002, Dubrovnik, Sept.2002, pp.1023-1026.
- [11] A.S. Kayhan, A. El-Jaroudi, L.F. Chaparro: "Data-Adaptive Evolutionary Spectral Estimation", *IEEE Trans. SP*, vol.43, no.1, Jan. 1995, pp.204-213.
- [12] S.Y. Kung, H.J. Whitehouse, T. Kailath: *VLSI and Modern Signal Processing*, Prentice-Hall, Inc., New Jersey, 1985.
- [13] M. T. Özgen: "Extension of the Capon's spectral estimator to time-frequency analysis and to the analysis of polynomial-phase signals", *Signal Processing*, 2003. in print (available at the publisher's www).
- [14] S. Peleg, B. Porat, B. Friedlander: "The achievable accuracy in estimating the instantaneous phase and frequency of a constant amplitude signal", *IEEE Trans. Sig. Processing*, Vol. 41, pp. 2216-2223, June 1993.
- [15] B.Ristic, B. Boashash: "Relationship between polynomial and higher order Wigner-Ville distribution", *IEEE Signal Processing Letters*, vol-2, no.12, Dec. 1995, pp.227-229.
- [16] L.J. Stanković: "A method for improved distribution concentration in the time-frequency signal analysis using the L-Wigner distribution", *IEEE Trans. on Signal Processing*, vol-43, no.5, May 1995, 1262-1268.
- [17] P. Stoica, R.L. Moses: *Introduction to spectral analysis*, Prentice-Hall, Upper Saddle River, New Jersey, 1997.
- [18] P. Stoica, A.Jakobson, J. Li, "Matched-filter bank interpretation of some spectral estimators", *Signal Processing*, 66, 1998, pp. 45-59.